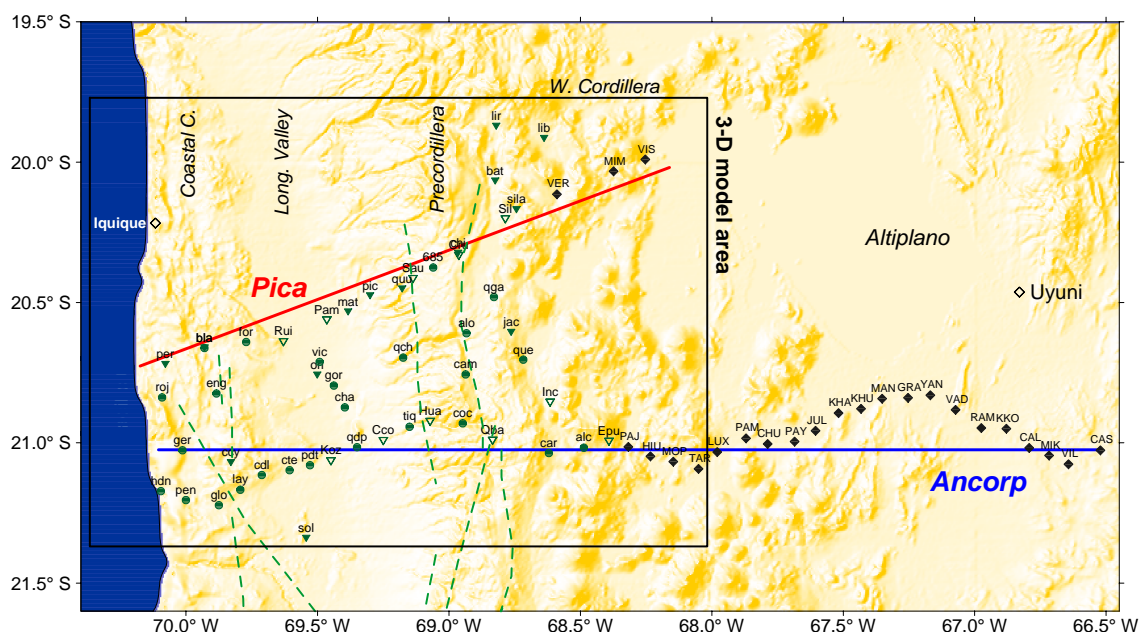


## Chapter 4

# Presentation of the study area



*Figure 4.1:* Presentation of the measured area showing the MT sites of the different campaigns. Dark diamonds are for the Bolivia 1997 campaign, dark circle for the Chile 1998, open and dark reversed triangles for the Chile 1993 and 1995 campaigns, respectively. The dark rectangle indicates the area planned for the 3-D modeling, as well as two classified profiles (Pica and Ancorp) for the 2-D modeling study. The broken lines indicate the main faults: in the Coastal Cordillera the "Atacama" fault system; in the Precordillera, the West Fissure.

MT measurements were carried out in the Southern Central Andes in four different campaigns (1997-1999) within the framework of the German Collaborative Research Programme SFB267 "Deformation Processes in the Andes", conforming two principal profiles: a northern one oriented WWS-EEN at latitude 20.5°S and a southern one oriented W-E at latitudes 21°S (Pica and Ancorp in fig. 4.1). The northern profile is located in the Coastal Cordillera (CC) and extends to the east over the volcanic arc of the Western Cordillera (WC). The southern profile region comprehends also the Coastal and Western Cordillera and extends to the east

to the eastern Altiplano (AP). The MT sites between both profiles will permit a 3-D modeling of the region, from the coast until the eastern margin of WC (longitudes  $68^{\circ}\text{W} - 70^{\circ}\text{W}$ ).

### Data acquisition and processing

MT data were registered with instrumental data loggers from FU and GFZ developed at the University of Göttingen by Steveling and Leven [1992]. The two horizontal electric field components were acquired with two pairs of electrodes with a spacing of 50 - 100 m. The unpolarizable electrodes contain KCL electrolyte and an Ag core. In the field they were buried with bentonite to lower the contact resistance and to stabilize the self potential. The horizontal and vertical magnetic field components were measured with a fluxgate magnetometer, designed by Magson GmbH (Berlin). The measured coordinate system was settled with respect to magnetic North; thus both horizontal components are EW and NS oriented.

MT measurements were carried out in four different campaigns (1993, 1995, 1997 and 1999), and all data were processed with the Egbert & Booker (1986) package. This processing is a robust single site method developed to calculate the electromagnetic transfer functions.

Prior to a Fourier transform, the time series of each electric and magnetic field component was cleaned up of isolated outliers with a running median filter. Sometimes bad data segments containing peaks were manually excluded from further processing. Data were pre-whitened within a decimation scheme (adapted by S. Friedel in 1997) by an autoregressive filter. Then, 128 Fourier coefficients were selected for the windowed transformation, yielding dense spectral estimates in the frequency domain. At last, the MT impedance tensor and the two magnetic transfer functions were calculated using the regression M-estimate described by Egbert and Booker [1986]. The range of the transfer functions is between 10 and 20000 s, and the errors for single periods are contained in a covariance matrix of 95% confidence limit.

Shorter period data in the 10-100 s band were most sensitive to bias due to low excitation energy. Using a remote reference station for the processing helped to reduce this effect. The remote reference stations were selected according to the various field campaigns, with a preference given for sites with a long operating time, thereby improving data quality.

The oldest 1993 and 1995 data campaign were re-processed by W. Soyer with the same procedure as mentioned above (Egbert and Booker [1986] package).

### Presentation of the data

The MT magnetic transfer functions will be presented in the impedance phase form<sup>1</sup>. The site data for the phases of the off-diagonal tensor elements are shown for each profile in W-E pseudo-sections as a function of the period (fig.4.2). Assuming that the regional structure is N-S oriented, as expected in the subduction zone of the Andean system, the data are presented in the measured coordinate system with the X-axis oriented in N-S. Some 2-D features can be qualitative recognized as a first approach.

In a 2-D approximation, the YX polarisation mode (and thus TM) is most sensitive to the lateral conductivity contrasts, since the electric field component across the structure decreases in the media of lower resistivity value. Also, the impedance phase of either XY (TE) or YX polarization mode increases when the fields penetrate into a less resistive medium in depth,

---

<sup>1</sup>Apparent resistivity data from selected sites will be presented in further chapters.

or decreases if the medium becomes more resistive (section 1.1).

The right column of Fig.4.2 shows the phase pseudo-sections of the YX polarization mode for the north (Pica), central and the south (Ancorp) profiles (fig.4.1), i.e., the phase differences between the W-E electric field and the N-S magnetic field components. The violet and blue colors indicate low phase values, whereas colors from yellow to red indicate high phase values increasing between  $50^\circ$  and  $90^\circ$ . Phases surpassing  $90^\circ$  are in white.

The very low TM-phase values observed between the Coastal Cordillera (CC) and the Precordillera ( $70^\circ$  to  $69^\circ$ W) are an evident coast effect. The ocean in this region reaches depths of 4-8 km (section 9.1), associated with a high conductivity of about 3.3 S/m (e.g., Schwarz and Krüger [1997]).

To the east (WC and Altiplano), an increment of the phase with period (square root proportional to the penetration depth) is an indication of lower resistivity values in depth. The white areas at the longest periods in the Ancorp profile express bad data quality, where phase errors are large. The same situation occurs at the shorter period data at site MAT and CCY on the Pica and the central profile, respectively. It can be inferred from the pseudo-sections that the most remarkable 2-D effect is the ocean effect, where the coast line extends approximately N-S. Another 2-D feature can be recognized at longitude  $69^\circ$ W, where the Precordillera begins to the east. This could be reflecting the attenuation of the coast effect and the beginning of another effect such as a high conductivity zone to the east.

In the pseudo-sections of the XY-polarization mode (fig.4.2; left), the phases are in contrast much distorted at the site data located in the Coastal Cordillera ( $70^\circ$ W to  $69.5^\circ$ W) and Precordillera ( $-69^\circ$ W). The white areas at different period bands are not a bad quality character of the data but an anomalous behaviour associated with strong current channeling effects (Section 6.3).

From the XY pseudo-sections (fig.4.2; left) we can also infer the 2-D feature at longitude  $69^\circ$ W, where to the east the phase increment with the period is again observed.

The magnetic transfer functions are presented in the induction arrow form with the Schmucker convention (Schmucker [1970]; arrows point toward to higher resistivity regions). Real and imaginary parts for three periods (100, 1300 and 7200 s) are shown in fig.4.3, representative for shallow, intermediate and great penetration depths, respectively.

The induction arrows allow a qualitative recognition of regional lateral conductivity variations (section 1.1) in the area, if no superposition by nearly conductivity anomalies exist. Thus the projection of them on the measured area map permits a 3-D overview as well.

In CC we can observe a very similar behaviour of the real arrows at shorter and longer periods. They are systematically deviated from the W-E direction as expected under a pure ocean effect. The systematical deviations are explained by the presence of another conductor in the Coastal Cordillera (associated with the Atacama fault system; chapter 7), which together with the ocean affects the magnetic transfer functions at almost all penetration depths. While the imaginary parts at shorter periods are relative perpendicular to the real parts, smaller angle departures from their respective real parts are in general observed at longer periods, thus reflecting a stronger 2-D effect at greater depths.

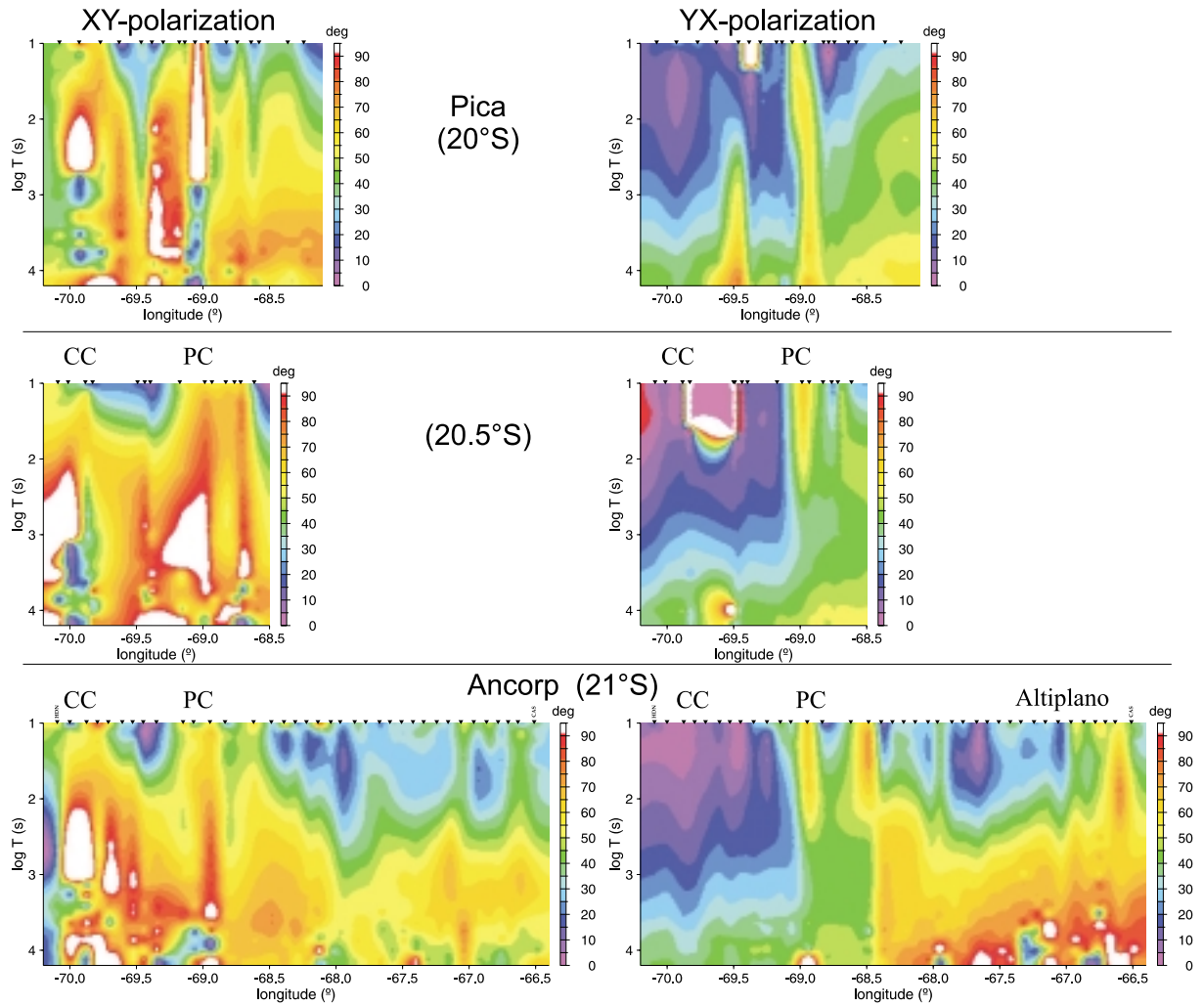


Figure 4.2: MT phase pseudo-sections of the **XY** (left) and **YX** (right) polarization mode of the two profiles shown in fig.4.1 and the sites in between ( $20.5^{\circ}\text{S}$ ). The sites are projected along W-E traverses. The vertical axis is the logarithm of the period (s). X is the geomagnetic north. **CC**, **PC**: Coastal and Pre-Cordillera.

To the east of CC, there is a reversal of the real induction arrows direction. The exception is observed at the longest periods, where they still point similarly as the CC arrows, which can be explained by the observation made above about the stronger CC 2-D effect in depth. Between the longitudinal valley (LV) and the Precordillera (PC), the shorter periods' real arrows are pointing away from the PC fault system in a 3-D manner (fig.4.3). Thus a high conductivity zone beneath the PC fault systems can be thought to be present. Nevertheless at greater penetration depths this 3-D effect becomes less significant, as observed in the decrement of the arrows length with period.

Between PC and WC the arrows change again in direction at long periods, turning to point more away from the east direction. In WC itself the real vectors tend to point in EW direction, reflecting a higher conductivity zone in the Altiplano (AP).

In the Precordillera it is not possible to recognize a regional 2-D feature, because the induction arrows strongly vary with the period. It seems that local 3-D structures must be coupled with more regional structures to the east and west of it, in order to explain the systematic

induction arrow deviations (chapter 8). This observation can also be supported by the strong angle departure and magnitude difference seen between the real and imaginary induction arrows.

The presented data will be considered in the modeling sections (chapter 9) after analyzing the dimensionality and the degree of distortion in them (chapters 5, 6.3).

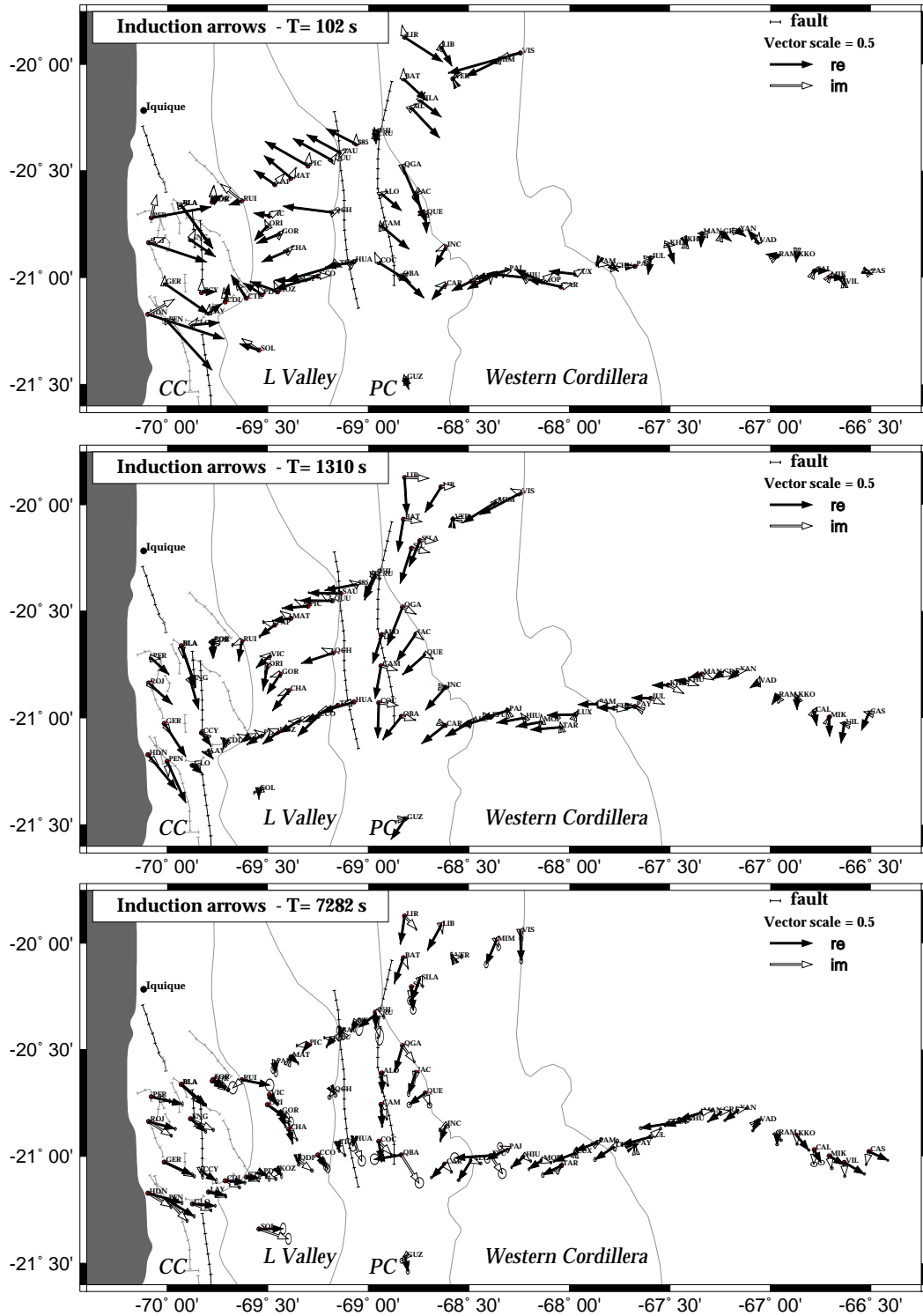


Figure 4.3: Real (black) and imaginary (white) parts of the induction arrows of the study area. Real parts point away of good conductors. Above: Representative for short penetration depths (100 s). Center: Intermediate penetration depths (1300 s). Below: Great penetration depths (7200 s). Ellipsoids indicate the measured errors. Also shown are the main fault systems of the region.